CrossMark

ORIGINAL PAPER

Long Wavelength Propagation of Elastic Waves Across Frictional and Filled Rock Joints with Different Orientations: Experimental Results

Resmi Sebastian · T. G. Sitharam

Abstract A study on long wavelength propagation of shear and compression waves across jointed rocks is important as this condition exists in field. Wave propagation velocities and damping of waves across a jointed rock mass depend on many factors and orientation of rock joints is one of them. The experimental study on influence of joint orientation during wave propagation is carried out using resonant column apparatus. The jointed Plaster of Paris samples with and without infill material have been used to simulate the jointed rock mass with different orientations. The experiments and analyses are centered on propagation of shear and compression waves in jointed rocks with different orientations. Wave velocities and wave attenuations across frictional and filled rock joints are obtained for different strain levels and confining pressures. The results show that propagation of shear waves is dependent on joint orientation. Shear waves are attenuated more than compression waves and confining pressure decreases this influence of joint orientation. Results show that filled joints can damp the waves more easily than frictional joints. The joints oriented perpendicular to direction of wave propagation are more effective in damping compared to joints oriented parallel to the direction of wave propagation.

1 Introduction

The wave characteristics influence the energy transmission across joints and vice versa. The presence of joints makes the rock medium as anisotropic and this in turn affects the velocity and damping of propagating seismic waves. Information on wave propagation characteristics are very important in the analysis of a jointed rock mass for subsurface exploration studies as well as for safety of the substructures constructed in them. The wave velocities and damping behavior describe the stiffness and stability of rock mass and wave propagation across joints in a rock mass has been a subject of research for many researchers. Study on velocity reduction of waves across joints is of prior importance in earth quake engineering. Linear and non-linear elastic deformation behavior of joints during wave transmission has been described by researchers, Miller (1978), Schoenberg (1980), Pyrak-Nolte et al. (1990) and Zhao et al. (2006), using analytical as well as numerical methods including the

R. Sebastian (✉) · T. G. Sitharam
Geotechnical Engineering Division, Department of Civil Engineering, Indian Institute of Science,
Bangalore 560012, India
e-mail: resmisebastian@gmail.com

T. G. Sitharam
e-mail: sitharam@civil.iisc.ernet.in

study on joint contact formation using micro mechanical models (Resende et al. 2010).

The wave frequency dependent behavior of jointed rock mass is important as the vibrations from different sources are associated with different wavelengths/frequencies and they introduce different ranges of strains in rock mass. The propagation of a dynamic wave across a joint in a jointed rock mass is a complex phenomenon. The relation of wavelength of propagating wave to the spacing between joints is an important parameter that is related to the amount of energy transmitted or reflected or absorbed at the joints. Long wavelength propagation ($\lambda \gg L$; where L, is the spacing between two joints and λ, the wavelength of propagating wave) is a common situation that exists in the field as seismic sources often produce low frequency vibrations. Waves associated with long wavelength propagations often may not detect the presence of joints (Fratta and Santamarina 2002) during their propagation across a jointed rock mass and are transmitted as in a continuum. Hence, an analysis of long wave length propagation across joints is important. However, very few researchers have attempted to conduct a study on this condition due to the difficulty in simulating the condition in laboratory. Fratta and Santamarina (2002) conducted a study on long wavelength propagation across aluminum oxide discs by developing a test device that can apply torsional vibrations on the testing samples and calculated shear wave velocities from the resonant frequencies obtained. Cha et al. (2009) extended the study of Fratta and Santamarina (2002) to compression waves passing through gneiss, acetal and dental gypsum discs; and also by obtaining the damping of waves across joints. Mohd-Nordin et al. (2014) conducted studies with quasi static resonant column developed by Fratta and Santamarina (2002) using multi jointed cylindrical discs made of dental gypsum and correlated the wave propagation characteristics to joint roughness coefficient. Shear wave propagation study on jointed biocalcarenite rock (a type of sedimentary carbonate rock) samples was performed by Perino (2011) using a resonant column apparatus (RCA).

Wave velocities and attenuation/damping of waves across joints depend not only on the number of joints and spacing of joints; but also on the orientation of joints in rocks (Wu et al. 1998; Ramulu 2009). Previous studies conducted on long wavelength propagation across jointed rocks (Fratta and Santamarina 2002; Cha et al. 2009; Perino 2011; Mohd-Nordin et al. 2014) are constrained to horizontal joints at a particular strain level. Hence, a study on the influence of orientation of joints becomes an important one. A jointed rock mass may be subjected to different types of vibrations due to blasting, earth quakes, traffic loads, nearby constructions etc. These vibrations impart strain levels of various ranges. Moreover, the confining pressures that rocks are subjected to also influence the wave velocities and damping behavior.

Joints that exist in a rock mass may be frictional joints or filled joints. Joints in a rock mass that contain gouge materials in them are referred to usually as filled joints. Similarly the rock joints that do not have any filling material in between are known as frictional joints. Long-wave length propagation of shear and compression waves across frictional and filled joints has been simulated in the laboratory. A comprehensive experimental study involving velocities as well as damping/attenuation behavior of waves over various strain levels and confining pressures, has been conducted for various joint orientations and the results are presented in this paper.

2 Methodology

Study on influence of joint orientations on wave velocities and damping behavior was conducted using a RCA on Plaster of Paris samples (POP). Adopting model materials for conducting studies in rock mechanics is very common as obtaining rock samples for studies are practically difficult and expensive. Brown and Trollope (1970) developed strength envelope for jointed rock mass after obtaining shear strength parameters for various joint orientations, by conducting series of triaxial compression tests on jointed samples developed using plaster cubes. As the behavior of hardened POP is similar to that of soft rock, Ramamurthy and Arora (1994) used POP samples for conducting studies on rocks whereas Cha et al. (2009) used dental gypsum discs for studying rock behavior during wave propagation by obtaining shear and compression wave velocities across them. Indraratna and Haque (2000) used gypsum plaster as model material for conducting study on shear behavior of rock joints. POP was chosen for the study as the samples are easily reproducible and are less stiff than actual rock samples so

that they fall within the stiffness specifications of RCA. They are easier to prepare and economical. Cylindrical POP samples of dimensions 50 mm diameter and 100 mm length (dimensions required for RCA testing) were prepared by pouring POP–water mix (at a fixed POP–water ratio) into prefabricated split moulds and removing the set samples after few hours. Then, the samples were dried under normal room temperature and humid conditions for 12–14 days to attain constant weight. A cutter was used to create joints in various directions. To simulate filled joints, kaolinite mixed with water at its plastic limit water content (PL = 35 %) was filled in the joints of POP samples at 2 mm thickness. The mechanical properties of the prepared POP samples and the infill material are given in Table 1.

A resonant column apparatus is usually used to obtain the low strain dynamic properties of materials. The system (RCA) is developed on the principle that resonant frequencies of sample (in torsion and flexure) can provide the shear and compression wave velocities while the strains induced in the sample are in the elastic range. Corresponding to each apparatus, there is a range to the amplitude of vibrations that can be applied to the samples, to obtain the resonant frequency of samples at various strain levels, but always within the elastic range. The apparatus used for the present study was able to measure the resonant frequencies of POP samples within the strain range of 5×10^{-5} %–1×10^{-2} %.

The RCA used for study is presented in Fig. 1a, b. The apparatus has its boundary conditions as bottom

Table 1 Properties of materials used for study

Properties of POP samples	Values
Density (kg/m^3)	1070
Cohesion (MPa)	0.5
Angle of internal friction (°)	65
Uniaxial compressive strength (MPa)	4.165
Poisson's ratio	0.29
Young's modulus (GPa)	4.5
Properties of kaolinite	Values
Specific gravity	2.6
Plastic limit (%)	35
Mean particle diameter (m)	2.6×10^{-7}

fixed and top free with additional masses attached to the free end. Shear wave velocities are measured using torsional vibrations produced by the electromotive force (EMF) generated due to the movement between four sets of magnets and coils. These vibrations are applied to top of the sample. The bottom of the sample is fixed to the base platen. The sample is vibrated at its fundamental mode of vibration by varying the frequency of vibrations at particular strain level. Resonant frequency is evaluated from these experiments and from the natural frequency (resonant frequency) thus obtained for each strain level, shear wave velocity is calculated. The theory of calculating shear wave velocities from torsional vibrations is explained below (Richart et al. 1970). The presence of additional masses like driving plate, accelerometer and top plate on top of sample alters the fixed—free boundary condition and mass polar moments of inertia of additional masses placed on top of sample are accounted in the calculation of shear wave velocities as:

$$V_s = \frac{2\pi fl}{\beta} \tag{1}$$

where $\beta \tan\beta = I/I_0$; I, I_0 = mass polar moment of inertia of specimen and driving plate respectively, V_s = shear wave velocity, f = resonant frequency of specimen obtained from resonant column test and l = length of specimen tested.

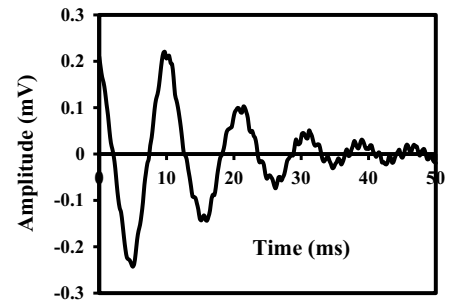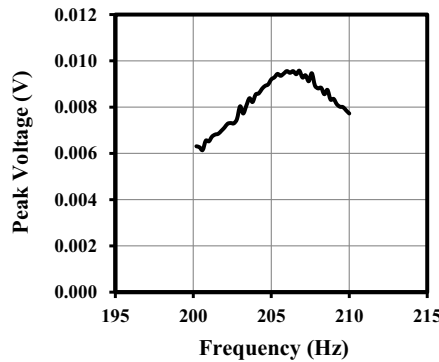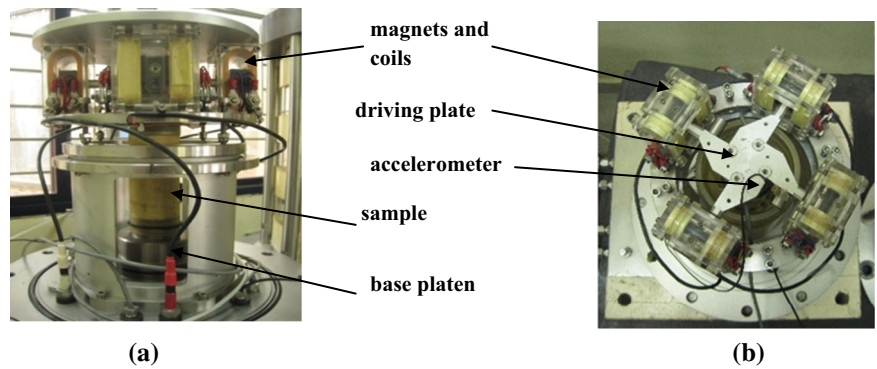The wavelength, λ of the propagating wave is calculated from;

$$\lambda = V_s/f. \tag{2}$$

For developing flexural vibrations, two alternate coils are switched off and the other two sets of magnets and coils induce a horizontal force to top of the sample. The whole system involving specimen and driving plate are assumed elastic with a lumped mass at the end of specimen. It is considered that the total energy of the system remains constant as the system is elastic and the principle behind application of flexural vibrations using RCA can be explained using Rayleigh's Energy Method (Cascante et al. 1998). By varying the amplitude of flexural vibrations applied to the sample, resonant frequencies at various strain levels can be obtained. As the bottom of the system (involving the specimen and lumped mass) is considered fixed, the displacement of the system

Fig. 1 a Resonant column apparatus (*front view*), **b** RCA (*top view*), **c** Resonant frequency curve, **d** Free vibration damping curve

(a)

(b)

(c)

(d)

linearly varies from zero (at bottom) to the maximum (at top). From the flexural resonant frequency, Young's modulus is obtained as

$$E = \frac{\omega_f^2}{3I_b}\left[\frac{33}{140}m_T + \sum_{i=1}^{n} m_i h(h0_i, h1_i)\right]l^3 \quad (3)$$

where $\omega_f = 2\pi f_v$ with f_v = flexural resonant frequency obtained E = Young's modulus of specimen I_b = area moment of inertia of specimen m_T = mass of specimen, m_i = mass of each additional mass placed on top of sample (i = 1,2,…) and $h(h0_i, h1_i)$ in (3) is obtained as:

$$h(h0_i, h1_i) = 1 + 3\frac{(h0_i + h1_i)}{2l} + \frac{3}{4}\left(\frac{h0_i^2 + h1_i h0_i + h1_i^2}{l^2}\right). \quad (4)$$

Young's modulus calculated from the formula (3) gives the longitudinal wave velocity in a bounded medium as,

$$V_{rod} = \sqrt{\frac{E}{\rho}} \quad (5)$$

In order to obtain the body P wave velocity, the use of Poisson's ratio is inevitable.

$$V_{p-body} = V_{rod}\sqrt{\frac{(1-v)}{(1+v)(1-2v)}} \quad (6)$$

where v is Poisson's ratio obtained from resonant column test as:

$$v = 0.5\frac{V_{rod}^2}{V_s^2} - 1. \quad (7)$$

Calculation of Poisson's ratio from wave velocities is valid only when the material is homogenous, isotropic and linearly elastic. As jointed rock samples are anisotropic and heterogenous, Poisson's ratio calculated from wave velocities are not valid (Thomsen 1990) and may give negative values or values >0.5. Hence the use of Poisson's ratio is avoided for

the analyses and compression wave velocity is assumed the same as that of longitudinal wave velocity for bounded medium in this study. From the wave velocity thus obtained, the wavelength of propagating wave is calculated using (2). The shear modulus of the sample is calculated from V_s, using $G = \rho V_s^2$ (ρ = density of material) and Young's modulus is obtained directly from (3).

Free vibration damping curve can be obtained for samples both in torsion and in flexure using a RCA. The sinusoidal vibration is applied to the sample and the excitation is suddenly shut off so as to produce free vibration to the sample tested. The accelerometer attached to the driving plate picks up the vibrations and free vibration damping curves are produced. The logarithmic decrement obtained from the free vibration damping curve can give out the damping ratio (D) and attenuation coefficient.

The logarithmic decrement, δ is obtained as:

$$\delta = \ln\frac{z1}{z2} \tag{8}$$

where z1 and z2 are two successive amplitudes of the free vibration damping curve.

The damping ratio, D is calculated as:

$$D = \sqrt{\frac{\delta^2}{4\pi^2 + \delta^2}} \tag{9}$$

The attenuation coefficient, α, is then obtained from (Richart et al. 1970), $\alpha = \delta/\lambda$.

A typical resonant frequency curve and a free vibration damping curve are shown in Fig. 1c, d respectively. The peak frequency which is the resonant frequency obtained from the frequency curve is used to obtain the wave velocities during the analyses.

3 Suitability of Using RCA for Rock Mechanics Studies

Resonant column apparatus is used usually for obtaining the wave velocities and moduli of soils. By incorporating few modifications to the testing method and by applying corrections to the obtained wave velocities, stiff samples (within the stiffness limits of the equipment) also could be tested with the apparatus. The vital issues that come up in testing stiff samples in a RCA are fixity conditions (insufficient

fixity of base), insufficient coupling of samples at end platens, over estimation of damping and under estimation of wave velocities (Drnevich 1978), generation of back EMF leading to over estimation of damping (Cascante et al. 2003; Wang et al. 2003) and over stiffness of samples (Drnevich 1978; Kumar and Clayton 2007). The fixity of bottom pedestal of RCA was checked against conditions, given out by ASTM D4015-92 (2000) and Ashmawy and Drnevich (1994), and it was found to be sufficient. The slippage of samples from end platens may lead to under estimation of wave velocities and over estimation of damping characteristics. Proper fixing of the samples to the end platens was ensured by the usage of epoxy resins (Khan et al. 2008) at the ends of samples and slippage of the samples from end platens could be avoided by this process.

Over stiffness of samples may lead to under estimation of resonant frequencies (Kumar and Clayton 2007). This problem could be solved by applying some corrections to the obtained resonant frequencies. These corrections were calculated using aluminum calibration bars of varying stiffness and resonant frequencies. The desired frequencies were back calculated from the known values of shear and compression wave velocities of aluminum bars. The obtained frequencies and desired frequencies were compared and relationship between them was established (Table 2) and was used to obtain correction factors for the analyses (Fig. 2).

The generation of an opposing EMF (back EMF) due to the changes in magnetic flux leads to over estimation of damping characteristics. RCA has the provision of an open circuit that is enabled during a free vibration (used for damping test) and this mechanism solves the difficulty caused due to back EMF.

4 Experimental Studies

POP samples with frictional and filled joints aligned in various orientations were used for conducting the study. Various orientations of joints that were used are 0°, 30°, 50°, 70° and 90°. The samples prepared to conduct the study on frictional joints are shown in Fig. 3a; and the samples with filled joints are shown in Fig. 3b. Figure 4 presents the notation for orientation of joints employed in resonant column tests.

Table 2 Actual and obtained resonant frequencies

Shear wave measurement				Compression wave measurement			
Diameter of bar (mm)	Obtained frequency (Hz)	Actual frequency (Hz)	Correction	Diameter of bar (mm)	Obtained frequency (Hz)	Actual frequency (Hz)	Correction
10	41.2	41.2	1	10	25	25	1
12.5	62.5	62.5	1	12.5	37.6	37.6	1
15	90	90	1	15	52.4	52.4	1
20	154	161.44	1.048312	20	91.1	100.1	1.098793
22.65	190.4	208.4	1.094538	22.65	114	128.3	1.125439
26.5	236.1	285.42	1.208895		135.48	175.4	1.294656

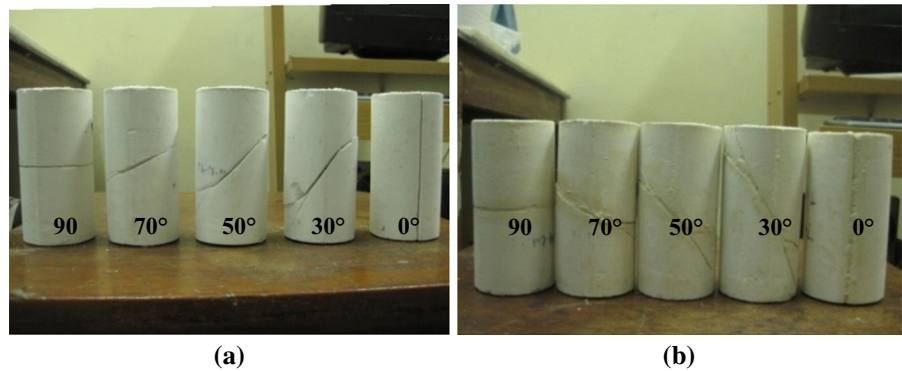**Fig. 2** Correction factors for **a** shear wave, **b** compression wave
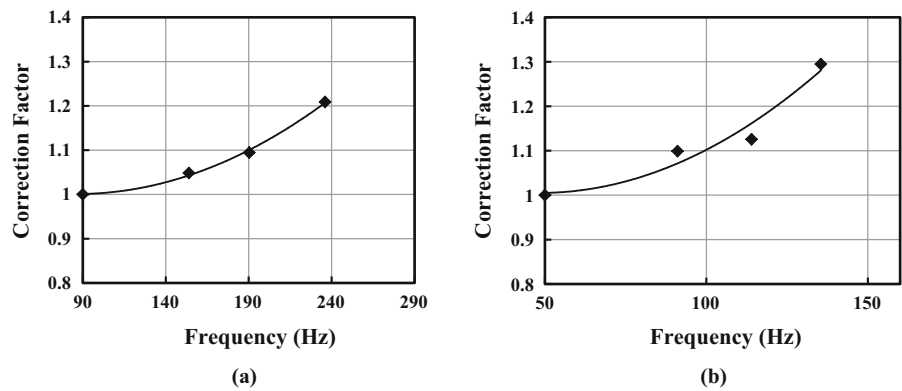
Fig. 3 **a** Frictional joints aligned in various orientations, **b** Filled joints aligned in various orientations

Resonant frequency tests were carried out on frictional and filled joints by varying the frequencies applied to the samples and picking the maximum frequency at different strain levels. Shear and compression wave velocities and damping curves were obtained for all joint orientations. All of these tests were performed under three different confining pressures (100 kPa, 300 kPa and 500 kPa) to analyze the influence of depths on these joint orientations. Confining pressures applied to the sample indicate the location of sample insitu and represent the all-round pressure sample experiences at field. The application of these low confining pressures thus denotes the near surface conditions that the sample experience.

Fig. 4 Notation for joint orientation used in tests
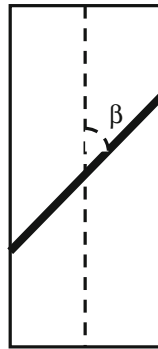
5 Results and Discussions

5.1 Wave Velocities

Shear and compression wave velocities were obtained under different strain ranges (2.5×10^{-4} %–8×10^{-3} % for shear waves and 1.5×10^{-4} %–1×10^{-2} % for compression waves) at various confining pressures. The wave velocity reduction curves for specimens with frictional joints corresponding to a confining pressure of 100 kPa for various orientations of joints are shown in Fig. 5a, b. Similarly, the responses of specimens with filled joints are also shown in Fig. 6a, b.

The plots clearly indicate that wave velocities reduce with increasing strain levels. Wave velocities are at maximum when the orientation of joint is vertical (0°) and are at minimum with horizontal joints (90°). It is observed that the response of joints on wave propagation depend much on their orientation, especially for shear waves. There is a uniform reduction in wave velocities as the orientation of joints vary from 0° to 90°. But for compression waves, the wave velocity reduction curve

of 0° joint stands apart from that of joints with other orientations. Wave velocity reduction curves of all other joint orientations are close and do not show much difference in wave velocities with varying joint orientations. The direction of application of flexural vibrations to the sample might have also contributed towards the enhancement in compression wave velocity for the sample with vertical joint. The joint would have experienced maximum stiffness as the vibrations were applied in direction (horizontal) that favored tight closure of joint.

Figure 7a, b show the shear wave velocity reduction across frictional joints for confining pressures of 300 kPa and 500 kPa respectively. The plots indicate that specimen with joint orientation of 0° has the maximum wave velocities for both confining pressures. It can be generalized from plots that the velocity reduction curves get closer and velocities increase as confining pressures increase. This may be due to the increase in the stiffness of joints with higher confining pressures. Figure 8a, b show the compression wave velocity reduction across frictional joints for confining pressures of 300 kPa and 500 kPa respectively. It is observed that the wave velocities across vertical joints always remain high above that of other joint orientations irrespective of changes in confining pressure. As confining pressures increase, joints of different orientations behave alike and waves are transmitted with almost same velocities, with the exception of vertical joints. However, an enhancement in velocities is always observed with increasing confining pressures.

The responses of specimens with filled joints for confining pressures of 300 kPa and 500 kPa are presented in Figs. 9 and 10. The shear and
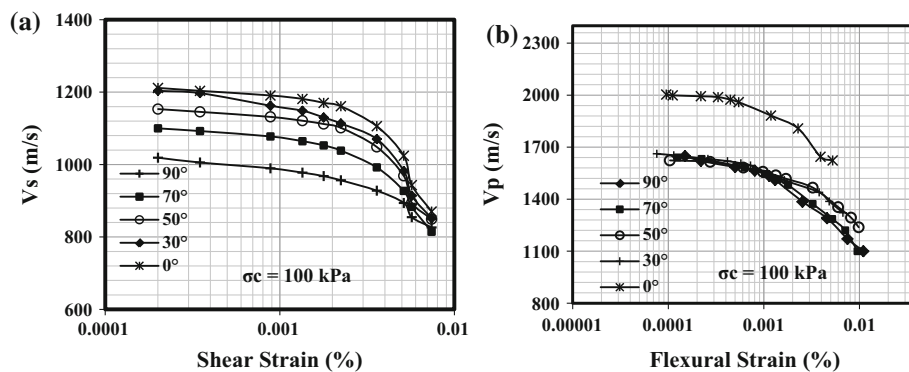

Fig. 5 Wave velocity reduction curves for specimens with frictional joints, **a** shear waves, **b** compression waves
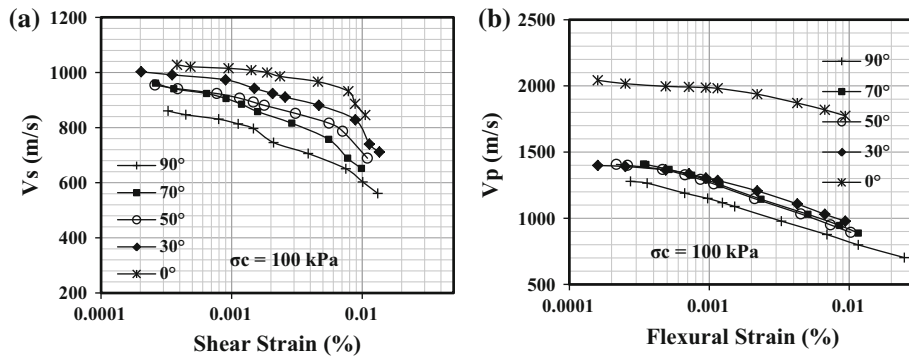
Fig. 6 Wave velocity reduction curves for specimens with filled joints, **a** shear waves, **b** Compression waves
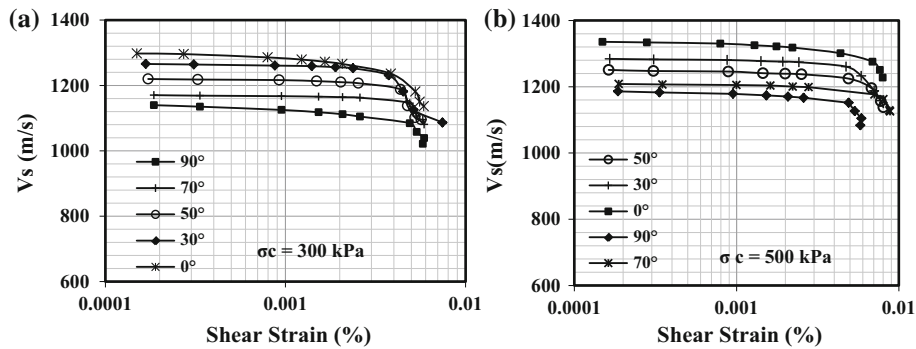

Fig. 7 Shear wave velocity reduction curves for specimens with frictional joints for confining pressures. **a** 300 kPa, **b** 500 kPa
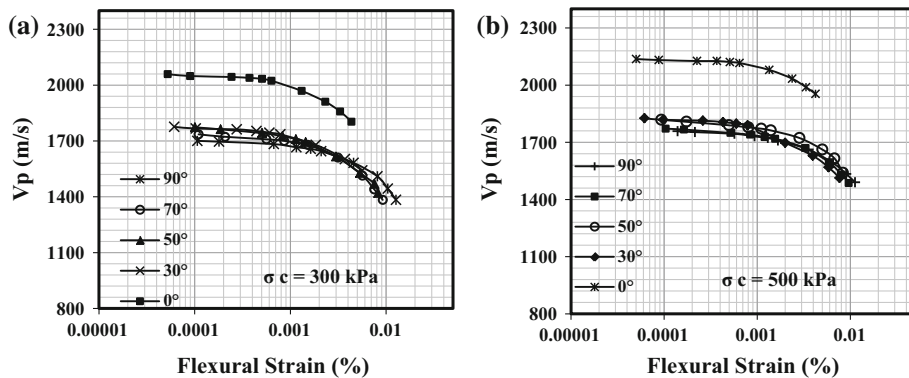

Fig. 8 Compression wave velocity reduction curves for specimens with frictional joints for confining pressures. **a** 300 kPa, **b** 500 kPa

compression wave velocity reduction patterns of specimens with filled joints across various joint orientations remain same as that of frictional joints. However the wave velocities of specimens with filled joints are always smaller than that with frictional joints due to the presence of gouge material in between the joints. The presence of infill material reduces the stiffness of joint considerably resulting in

low wave velocities. The increase in wave velocities with increasing confining pressures is also observed always, as for frictional joints.

5.2 Damping and Attenuation of Waves

Damping ratio is a measure of the energy dissipated during wave propagation. As mentioned by Cha et al.
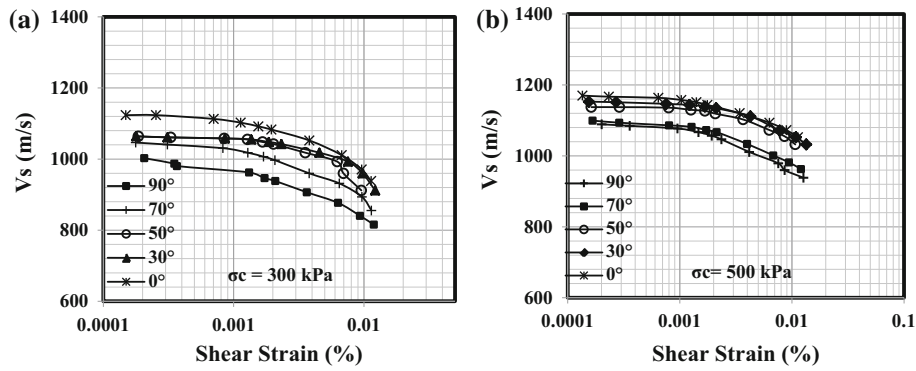
Fig. 9 Shear wave velocity reduction curves for specimens with filled joints for confining pressures. **a** 300 kPa, **b** 500 kPa
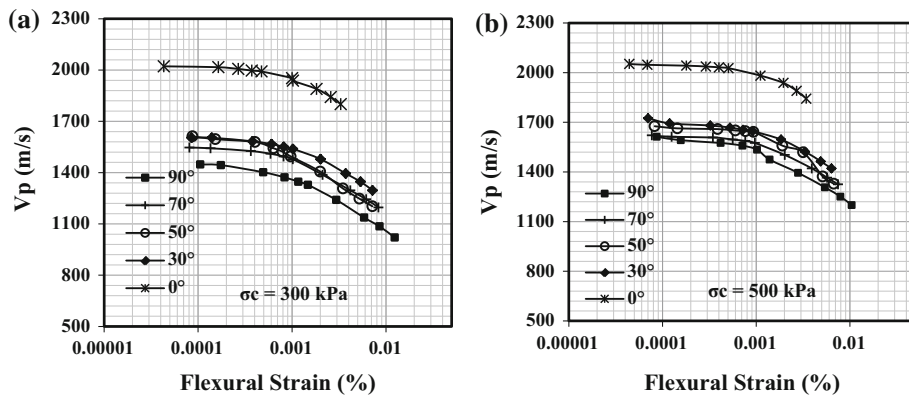

Fig. 10 Compression wave velocity reduction curves for specimens with filled joints for confining pressures. **a** 300 kPa, **b** 500 kPa

(2009), damping mechanism in a rock mass is controlled mainly by joints present in them. The amplitudes of the successive peaks of free vibration curve provide the logarithmic decrement which describes the viscous damping. Usage of logarithmic decrement is only intended to describe the damping behavior of rocks, which is similar to viscous damping. Similarly, attenuation coefficient is also a measure of energy dissipation, that takes into consideration the wave length of propagating wave.

Figure 11a, b show the damping ratios obtained for frictional joints aligned in various orientations across different strain levels. The plots indicate that horizontal joints damp the waves most and vertical joints damp the least. It is also seen that the damping ratios always increase as strain levels increase. The attenuation coefficients calculated for shear and compression waves for specimens with frictional joints at strain level of 8×10^{-3} % for a confining pressure of

100 kPa are shown in Table 3. It is observed that shear waves attenuate almost twice that of compression waves. This difference in attenuation coefficients is due to the difference in the wavelengths of shear and compression waves. The trend of increasing wave attenuation with increasing strain levels is same as that of damping ratios as the attenuation coefficients are calculated from the logarithmic decrement of free vibration damping curve.

Figure 12a, b illustrate the damping ratios obtained across filled joints at a confining pressure of 100 kPa. It is observed that filled joints damp both shear and compression waves easily than frictional joints. The damping ratios obtained indicate that the damping effect of filled joints is almost twice that of frictional joints. The attenuation of waves across filled joints also follows the same trend of frictional joints that shear waves are attenuated more than compression waves.
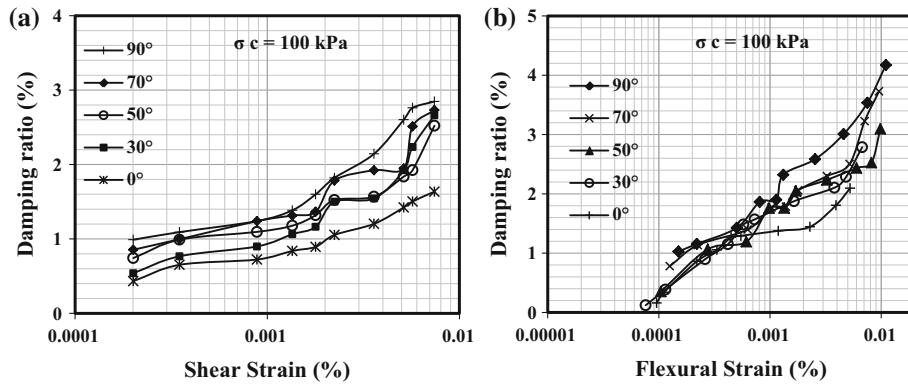
Fig. 11 Damping ratios for specimens with frictional joints. **a** shear waves, **b** compression waves

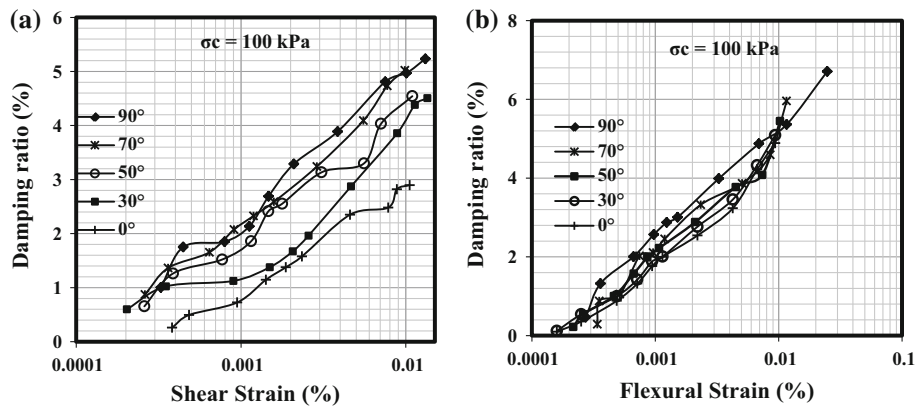| Table 3 Attenuation coefficients across frictional joints aligned in various orientations	Orientation of frictional joint	Attenuation coefficient, α for shear wave (/m)	Attenuation coefficient, α, for compression wave (/m)
	90°	0.038	0.021
	70°	0.036	0.018
	50°	0.034	0.015
	30°	0.034	0.014
	0°	0.022	0.010

Fig. 12 Damping ratios for specimens with filled joints. **a** shear waves, **b** compression waves

It is seen that attenuation/damping of shear waves are more dependent on orientation of joints, both for frictional joints and filled joints. Even though damping curves for all the joint orientations are close for compression wave, a close examination of plots reveals that samples with horizontal joints have high damping/attenuation potential than samples with other joint orientations. Figure 13a, b show the damping ratios obtained in shear and flexure for filled joints at a

confining pressure of 500 kPa. It could be observed that increase in confining pressures decrease the damping ratios due to the improved joint stiffness at higher confining pressures. This implies that waves are less damped at great depths than at shallow depths. As the behavior of frictional and filled joints is alike in this consideration, the damping curves of shear and compression waves for filled joints are only shown. It is very well noted that even for confining pressure of 500 kPa,
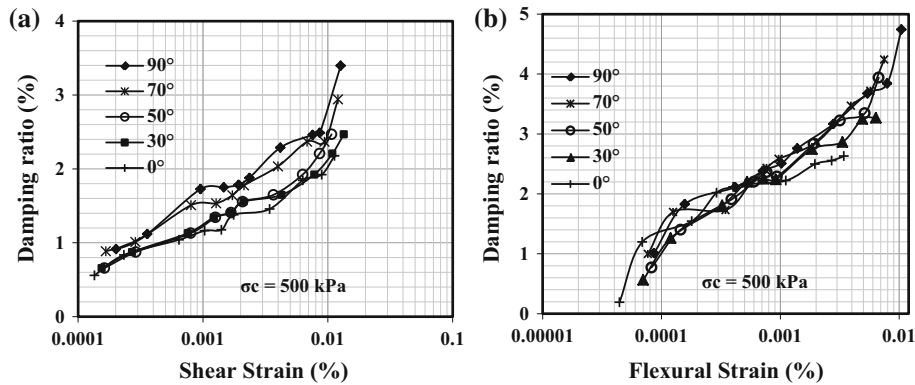
Fig. 13 Damping ratios for specimens with filled joints for confining pressure of 500 kPa. **a** shear waves, **b** compression waves

that damping ratios obtained for compression waves are less dependent on orientations of joints than shear waves.

6 Conclusions

A study on long wave length propagation of shear and compression waves across joints of various orientations has been performed using RCA. Experiments on frictional and filled joints were conducted and influence of obliquely oriented joints on wave propagation velocities and damping ratio/attenuation coefficients were obtained for a range of strain levels.

Wave velocities obtained from tests conducted on the significance of joint orientations clearly indicate that rock masses with horizontal joints have lowest wave velocities across them. Rocks with perpendicular joints (joints aligned in the same direction of wave propagation) have highest wave velocities across them. Shear waves are influenced more by the orientation of joints than compression waves. Analyses have proved that the same situation exists for all confining pressures, but wave velocities increase as confining pressures increase. With the exception of vertical joints, joints aligned in any angle seemed to behave almost alike in compression wave velocity analyses.

The study on damping behavior of joints has indicated that waves propagated across samples with vertical joints are less damped and the waves propagated across samples with horizontal joints are more damped. Filled joints damp the waves more effectively than frictional joints and the shear waves are attenuated more than compression waves. Both frictional and filled joints with less confinement damp

shear and compression waves more easily at all strain levels.

References

Ashmawy AK, Drnevich VP (1994) A general dynamic model for resonant column/quasi static torsional shear apparatus. Geotech Test J 17(3):337–348

ASTM (D4015-92) (2000) Standard test methods for modulus and damping of soils by resonant column method. Annual book of ASTM Standards, ASTM International

Brown ET, Trollope DH (1970) Strength of model of jointed rock. J Soil Mech Found Div 96(2):685–704

Cascante G, Santamarina C, Yassir N (1998) Flexural excitation in a standard torsional resonant column device. Can Geotech J 35:478–490

Cascante G, Vanderkooy J, Chung W (2003) Difference between current and voltage measurements in resonant—column testing. Can Geotech J 40(4):806–820

Cha M, Cho G, Santamarina JC (2009) Long wavelength P-wave and S-wave propagation in jointed rock masses. Geophyics 74(5):E205–E214

Drnevich VP (1978) Resonant Column testing: problems and solutions. Dyn Geotech Test STP-654:384–398

Fratta D, Santamarina JC (2002) Shear wave propagation in jointed rock: State of stress. Geotechnique 52(7):495–505

Indraratna B, Haque A (2000) Experimental and numerical modeling of shear behavior of rock joints. In: GeoEng 2000, an international conference of geotechnical and geological engineering, vol 1. Pennsylvania

Khan ZH, Cascante G, El-Naggar H (2008) Evaluation of the first mode of vibration and base fixity in resonant column testing. Geotech Test J 31(1):1–11

Kumar J, Clayton CRI (2007) Effect of sample torsional stiffness on resonant column results. Can Geotech J 44:221–230

Miller RK (1978) The effects of boundary friction on the propagation of elastic waves. Bull Seismol Soc Am 68(4):987–998

Mohd-Nordin MM, Song K, Cho G, Mohamed Z (2014) Long wavelength elastic wave propagation across naturally fractured rock masses. Rock Mech Rock Eng 47:561–573

Perino A (2011) Wave propagation through discontinuous media in rock engineering. Dissertation, Polytechnic University of Turin, Turin

Pyrak-Nolte LJ, Myer LR, Cook NGW (1990) Transmission of seismic waves across single natural fractures. J Geophys Res 95(B6):8617–8638

Ramamurthy T, Arora VK (1994) Strength predictions for jointed rocks in confined and unconfined states. Int J Rock Mech Min Sci Geomech Abstr 31(1):9–22

Ramulu M (2009) Rock mass damage due to repeated blast vibrations in underground vibrations. Dissertation, Indian Institute of Science, Bangalore

Resende R, Lamas LN, Lemos JV, Calçada R (2010) Micromechanical modeling of stress waves in rocks and rock fractures. Rock Mech Rock Eng 43:741–761

Richart FE Jr, Woods RD, Hall JR Jr (1970) Vibrations of soils and foundations. Prentice Hall Inc, New Jersey

Schoenberg M (1980) Elastic wave behavior across linear slip interfaces. J Acoust Soc Am 68(5):1516–1521

Thomsen L (1990) Poisson was not a geophysicist. Lead Edge 9(12):27–29

Wang YH, Cascante G, Santamarina JC (2003) Resonant column testing: the inherent counter EMF effect. Geotech Test J 26(3):342–352

Wu YK, Hao H, Zhou YX (1998) Propagation characteristics of blast induced shock waves in a jointed rock mass. J Soil Dyn Earthq Eng 17:407–412

Zhao XB, Zhao J, Hefny AM, Cai JG (2006) Normal transmission of S-wave across parallel fractures with coulomb slip behavior. J Eng Mech 132(6):641–650